Reaction with dioxygen of a Cu(I) complex of 1-benzyl-[3-(2′-pyridyl)]pyrazole triggers ethyl acetate hydrolysis: acetato-/pyrazolato-, dihydroxo- and diacetato-bridged Cu(II) complexes†

Jhumpa Mukherjee and Rabindranath Mukherjee*

Received 25th August 2005, Accepted 22nd December 2005
First published as an Advance Article on the web 11th January 2006
DOI: 10.1039/b512086a

A copper(I) compound [(L^2)Cu(MeCN)$_2$][ClO$_4$] (**1**) containing a new bidentate N-donor ligand L^2, 1-benzyl-[3-(2′-pyridyl)]pyrazole, derived from the condensation of HL^1 [HL^1 = 3-(2-pyridyl)pyrazole] and benzyl chloride, has been synthesized. Structural analysis reveals that in **1** the copper(I) centre is coordinated by a pyridine and a pyrazole nitrogen from L^2 and two MeCN molecules, providing a distorted tetrahedral geometry. Reaction of **1** with dioxygen in *N*,*N*′-dimethylformamide (dmf) at 25 °C and subsequent workup with MeCO$_2$Et afforded an acetato-/pyrazolato-bridged polymeric copper(II) compound [(μ-L^1)Cu(μ-O$_2$CMe)]$_n$ (**2**). Notably, the deprotonated form of HL^1 and MeCO$_2$$^-$ have originated from debenzylation of L^2 and hydrolysis of MeCO$_2$Et, respectively. The structural analysis of **2** reveals a near-planar $\{Cu_2(\mu\text{-}L^1)_2\}^{2+}$ core unit in which two adjacent Cu(II) ions are bridged by the deprotonated *N*,*N*-bidentate pyridylpyrazole units of two L^1 and each such $\{Cu_2(\mu\text{-}L^1)_2\}^{2+}$ unit is bridged by MeCO$_2$$^-$ in a monodentate bridging mode [Cu · · · Cu separations (Å): 3.9232(4) pyrazolate bridge; 3.3418(4) acetate bridge], providing a polymeric network. Careful oxygenation of **1** in MeCN led to the isolation of a dihydroxo-bridged dicopper(II) compound [{(L^2)Cu(μ-OH)(OClO$_3$)}$_2$] (**3**). Interestingly, complex **3** brings about hydrolysis of MeCO$_2$Et under mild conditions (dmf, *ca.* 60 °C), generating a bis-μ-1,3-acetato-bridged dicopper(II) complex, [{(L^2)Cu(dmf)(μ-O$_2$CMe)}$_2$][ClO$_4$]$_2$·dmf·0.5MeCO$_2$H (**4**). Compounds **3** and **4** have $\{Cu_2(\mu\text{-}OH)_2\}^{2+}$ [Cu · · · Cu separation of 2.8474(9) Å] and $\{Cu_2(\mu\text{-}O_2CMe)_2\}^{2+}$ cores [Cu · · · Cu separation: 3.0988(26) and 3.0792(29) Å (two independent molecules in the asymmetric unit)] in which each Cu(II) centre is terminally coordinated by L^2. A rationale has been provided for the observed debenzylation of L^2 and hydrolysis of MeCO$_2$Et. The intramolecular magnetic coupling between the Cu^{II} ($S = 1/2$) ions was found to be ferromagnetic ($2J = 82$ cm^{-1}) in the case of **3**, but antiferromagnetic for **2** ($2J = -158$ cm^{-1}) and **4** ($2J = -96$ cm^{-1}). Absorption and EPR spectroscopic properties of the copper(II) compounds have also been investigated.

Introduction

Coordination chemistry of copper complexes is a subject of continuing importance[1] in connection with the structures and the reactivities of copper-containing metalloproteins.[2,3] Therefore, structural modulation of synthetic copper complexes by subtle perturbations of various multidentate N-donor ligands to understand the copper/dioxygen chemistry have attracted much interest over the past two-decades in relation with the biological systems and the potential applications in synthetic organic transformations.[4,5]

As part of our activity in bio-inspired coordination chemistry of copper (for example, modelling tyrosinase-like activity[6] and catechol oxidase activity,[7] and to characterize irreversibly oxidized products, from the reaction between copper(I) complexes and dioxygen[1a,6,7]) we have begun to target hydroxo-containing dicopper(II) complexes to develop biomimetic systems of hydrolases.[8–10] It is well known that a very common reactivity of copper(I) complexes with dioxygen is the formation of irreversibly oxidized product, bis-μ-hydroxo-bridged dicopper(II) complexes.[1a,11–13] Recently we demonstrated the nucleophilic reactivity of copper(II)-coordinated hydroxide ion, due to reactions of dioxygen with copper(I) complexes of symmetrical/unsymmetrical tridentate (2-pyridyl)alkylamine ligands, affording μ$_3$-carbonato-bridged tricopper(II) complexes.[14]

Inspired by the recent developments on the use of bidentate ligands[5,15] to investigate the reactivity property of copper(I) complexes with dioxygen, given literature reports on hydrolysis of amides/esters by copper(II) coordinated hydroxide ion[16,17] and our own experience on nucleophilic reactivity of copper(II) coordinated hydroxide ion[14] our present endeavour is set. Here we report on new chemistry utilizing a copper(I) complex, [(L^2)Cu(MeCN)$_2$][ClO$_4$] (**1**) of a bidentate ligand, 1-benzyl-[3-(2′-pyridyl)]pyrazole, which led, to the best of our knowledge, to the discovery of the first nonenzymic hydrolysis of an unactivated

---

Department of Chemistry, Indian Institute of Technology Kanpur, Kanpur 208 016, India. E-mail: rnm@iitk.ac.in; Fax: +91-512-2597437; Tel: +91-512-2597437

† Electronic supplementary information (ESI) available: ^{1}H NMR spectrum of (**1**) in CD$_3$CN. EPR spectrum (polycrystalline sample) of (**2**) at 120 K. UV-VIS spectrum of (**3**) in MeCN. UV-VIS spectrum of (**4**) in MeCN. EPR spectrum (polycrystalline sample) of (**4**) at 300 K. See DOI: 10.1039/b512086a

ester $MeCO_2Et$ by an isolated copper(II)-coordinated hydroxide ion, as a nucleophile. Thus, reaction of **1** with dioxygen in *N*,*N*′-dimethylformamide (dmf) at 25 °C and subsequent workup with $MeCO_2Et$ afforded an acetato-/pyrazolato-bridged polymeric copper(II) compound $[(\mu\text{-}L^1)Cu(\mu\text{-}O_2CMe)]_n$ (**2**) [HL^1 = 3-(2-pyridyl)pyrazole]. To shed light on the mechanism by which acetate is generated from the reaction between **1**, O_2 and $MeCO_2Et$ and to prepare the expected intermediate and a discrete acetato-bridged compound, we synthesized the dihydroxo-bridged dicopper(II) compound $[\{(L^2)Cu(\mu\text{-}OH)(OClO_3)\}_2]$ (**3**) and $[\{(L^2)Cu(dmf)(\mu\text{-}O_2CMe)\}_2][ClO_4]_2\cdot dmf\cdot 0.5MeCO_2H$ (**4**), respectively. This report presents the structural elucidation of compounds **1–4**, along with spectroscopic and detailed temperature-dependent magnetic behaviour of **2**, **3** and **4**.

Experimental

General considerations

All reagents were obtained from commercial sources and used as received, unless stated otherwise. Solvents were dried/purified as reported previously.[6,7,14] 3-(2-Pyridyl)pyrazole (HL^1)[18] and $[Cu(MeCN)_4][ClO_4]$[19] were prepared following reported procedures. All manipulations for the synthesis of the copper(I) complex were performed in an atmosphere of purified dinitrogen using standard Schlenk and glove box (Mbraun, Germany) techniques.

Synthesis of 1-benzyl-[3-(2′-pyridyl)]pyrazole (L^2). A mixture of benzyl chloride (0.872 g, 6.90 mmol), HL^1 (1 g, 6.90 mmol), benzene (80 cm^3), 40% aqueous NaOH (10 cm^3) and 40% aqueous tetra-*n*-butylammonium hydroxide (8 drops) was refluxed with stirring for 8 h and then stirred at room temperature for 12 h. The organic layer was then separated, washed twice with brine water, dried over anhydrous Na_2SO_4 and filtered. Solvent removal afforded a yellowish white solid (yield: 1.46 g, ~90%). 1H NMR (80 MHz; $CDCl_3$): δ 5.23 (2 H, s, CH_2), 6.87 (1H, d, pz H4), 7.25 (6H, m, py H5, bz H2,6), 7.66 (2H, m, py H3,4), 7.90 (1H, d, pz H5), 8.56 (1H, d, py H6).

Synthesis of copper complexes. $[(L^2)Cu^I(MeCN)_2][ClO_4]$ (1). To a degassed solution of L^2 (0.10 g, 0.43 mmol) in MeCN (10 cm^3) was added solid $[Cu(MeCN)_4][ClO_4]$ (0.14 g, 0.43 mmol). The resulting bright yellow solution was stirred for 30 min at room temperature. Then dry degassed Et_2O (10 cm^3) was added to the above solution. The yellow solid that precipitated was filtered, washed with a mixture (1 : 3, v/v) of MeCN/Et_2O and dried *in vacuo*. Single crystals suitable for structural studies were obtained by the diffusion of Et_2O into a MeCN solution of the complex under a dinitrogen atmosphere (yield: 0.160 g, ~78%). Found: C, 47.76; H, 4.14; N, 14.39. Calc. for $C_{19}H_{19}N_5O_4ClCu$: C, 47.50; H, 3.96; N, 14.58%. Molar conductance, Λ_M (MeCN, ~10^{-3} mol dm^{-3}, 298 K) = 130 Ω^{-1} cm^2 mol^{-1} (expected range[20] for 1 : 1 electrolyte: 120–160 Ω^{-1} cm^2 mol^{-1}). IR (KBr, cm^{-1}, selected peaks): 2250 (ν(CN) of MeCN; 1089 and 627 ($\nu(ClO_4^-)$). UV/VIS (MeCN), λ_{max}/nm (ε/dm^3 mol^{-1} cm^{-1}): 247 (22 600) and 283 (14 000). ^{1}H NMR (400 MHz, CD_3CN): δ 8.31 (1H, d, py 6-H), 7.99–7.91 (3 H, m, py 3,4-H and pz 3-H), 7.41 (1 H, t, bz 4-H), 7.22–7.21 (3H, m, bz 3,5-H and py 5-H), 7.11–7.10 (2H, d, bz 2,6-H), 7.00–6.99 (1H, d, pz 4-H), 5.23 (2H, s, $-CH_2Ph$), 2.18 (6H, s, CH_3CN).

$[(\mu\text{-}L^1)Cu^{II}(\mu\text{-}O_2CMe)]_n$ (2).

Method A. To a degassed solution of L^2 (0.10 g, 0.43 mmol) in MeCN (10 cm^3) was added solid $[Cu(MeCN)_4][ClO_4]$ (0.14 g, 0.43 mmol). The resulting bright yellow solution was stirred for 30 min at room temperature. Afterwards all the manipulations were performed in air, implying the essential participation of dioxygen in the synthesis of **2**. The solvent was then removed, dmf (3 cm^3) was added to the residue, and filtered. Vapour diffusion of $MeCO_2Et$ into the resulting solution afforded, after about a month, dark blue single crystals, suitable for structural analysis (yield: 0.03 g, ~26%). Found: C, 44.99; H, 3.45; N, 16.05. Calc. for $C_{10}H_9N_3O_2Cu$: C, 45.02; H, 3.38; N, 15.76%. IR (KBr, cm^{-1}, selected peaks): 1608 ($\nu_{asym}(MeCO_2^-)$), 1378 ($\nu_{sym}(MeCO_2^-)$). UV/VIS (Nujol mull), λmax/nm (ε/dm^3 mol^{-1} cm^{-1}): 267, 330, 645.

Method B. Solid $[Cu(H_2O)_6][ClO_4]_2$ (0.512 g, 1.38 mmol) was added to a stirred solution of HL^1 (0.200 g, 1.38 mmol) in MeOH (10 cm^3). The bluish green solution thus obtained was stirred for 30 min and to it a solution of Et_3N (0.140 g, 1.386 mmol) in MeOH (5 cm^3) was added dropwise. The solution was filtered to remove trace amounts of a precipitate and to it solid $MeCO_2Na$ (0.114 g, 1.390 mmol) was added, generating a deep blue solution. After 15 min the solid that separated was filtered, washed with MeCN and Et_2O and air-dried (yield: 0.270 g, ~74%). This product is identical to that obtained following *Method A*.

$[\{(L^2)Cu^{II}(\mu\text{-}OH)(OClO_3)\}_2]$ (3). To a degassed solution of L^2 (0.10 g, 0.43 mmol) in MeCN (10 cm^3) was added solid $[Cu(MeCN)_4][ClO_4]$ (0.14 g, 0.43 mmol). The resulting bright yellow solution comprising supposedly **1** was stirred for 10 min at room temperature. Exposure of this solution to dry O_2 did not bring about an immediate noticeable change in colour. However, on exposure of this solution to O_2 for 24 h, a green colour was generated, the green solution was allowed to slowly evaporate in air after discarding a minute amount of a greenish yellow solid that initially separated out. Dark blue crystals which formed within 2–3 days were filtered, washed with a mixture (1 : 3, v/v) of MeCN/Et_2O (4 cm^3) and dried *in vacuo* (yield: 0.075 g, ~43%). Found: C, 43.15; H, 3.56; N, 3.56. Calc. for $C_{30}H_{28}N_6O_{10}Cl_2Cu_2$: C, 43.37; H, 3.37; N, 10.12%. Molar conductance, Λ_M (MeCN, ~10^{-3} mol dm^{-3}, 298 K) = 240 Ω^{-1} cm^2 mol^{-1} (expected range[20] for 1:2 electrolyte: 220–300 Ω^{-1} cm^2 mol^{-1}). IR (KBr, cm^{-1}, selected peaks): 3550 ($\nu(OH^-)$), 1106 and 623 ($\nu(ClO_4^-)$). UV/VIS (MeCN), λmax/nm (ε/dm^3 mol^{-1} cm^{-1}): 245 (30 700), 295 (25 700), 648 (140).

$[\{(L^2)Cu(dmf)(\mu\text{-}O_2CMe)\}_2][ClO_4]_2\cdot dmf\cdot 0.5MeCO_2H$ (4). Dark blue crystals of complex **3** were dissolved in dmf (2 cm^3). To the resulting green solution was added dry $MeCO_2Et$ (5 cm^3), and warmed on a water bath at ~60 °C. After 4 h the bluish green solution was kept in a refrigerator. Within 24 h the light bluish green crystals that formed were collected by filtration and dried *in vacuo*. These crystals were found to be suitable for X-ray structural study (yield: 0.040 g, ~57%). Found: C, 45.14; H, 4.44; N, 10.98. Calc. for $C_{44}H_{55}N_9O_{16}Cl_2Cu_2$: C, 45.40; H, 4.73; N, 10.83%. Molar conductance, Λ_M (MeCN, ~10^{-3} mol dm^{-3}, 298 K): = 260 Ω^{-1} cm^2 mol^{-1}. IR (KBr, cm^{-1}, selected peaks): 1650 (ν(CO) of DMF)), 1580 ($\nu_{asym}(MeCO_2^-)$), 1439 ($\nu_{sym}(MeCO_2^-)$), 1106 and 627 ($\nu(ClO_4^-)$). UV/VIS (MeCN), λmax/nm (ε/dm^3 mol^{-1} cm^{-1}): 246 (40 150), 291 (31 300), 718 (130), 964 (60).

Caution: Perchlorate salts of compounds containing organic ligands are potentially explosive.

Physical measurements

Elemental analyses were obtained with a Carlo Erba CHNSO 1110 analyzer. Conductivity measurements were performed with an Elico type CM-82T conductivity bridge (Hyderabad, India). Spectroscopic measurements were made using the following instruments: IR (KBr, 4000–600 $\mathrm{cm^{-1}}$), Bruker Vector 22; electronic, Perkin Elmer Lambda 2 and Agilent 8453 diode-array spectrophotometer; X-band EPR, Bruker EMX 1444 EPR spectrometer operating at 9.455 GHz (fitted with a quartz Dewar for measurements at 120 K). The EPR spectra were calibrated with diphenylpicrylhydrazyl, DPPH ($g = 2.0037$).

Magnetism

Magnetic susceptibility measurements on solid samples of **3** were obtained in the solid state using a Quantum Design (Model MPMSXL-5) SQUID magnetic susceptometer operating at magnetic field of 1.0 T. Variable temperature (54–300 K for **2**; 60–300 K for **4**) magnetic susceptibility measurements on **2** and **4** in the solid state were performed using a locally-built Faraday balance[21] comprising an electromagnet with constant gradient pole caps (Polytronic Corporation, Mumbai, India), an ultravacuum Sartorius M25-D/S Balance (Germany), a closed-cycle refrigerator and a Lake Shore temperature controller (Cryo Industries, USA). All measurements were made at a fixed main field strength of ~0.6 T. Solution-state magnetic susceptibilities were obtained by the NMR technique of Evans[22] in MeCN with a PMX-60 JEOL (60 MHz) NMR spectrometer. Corrections underlying diamagnetism were applied with use of appropriate constants.[23] Effective magnetic moments were calculated from $\mu_{\mathrm{eff}} = 2.828\,[\chi_{\mathrm{M}}T]^{1/2}$, where χ_{M} is the corrected molar susceptibility.

Crystal structure determinations

X-Ray data were collected on a Bruker SMART APEX CCD diffractometer, with graphite-monochromated Mo-K_α ($\lambda = 0.71073$ Å) radiation at 100(2) K. For data reduction the 'Bruker Saint Plus' program was used. Data were corrected for Lorentz and polarization effects; empirical absorption correction (SADABS) was applied. Structures were solved by direct methods using SIR-97 and refined by full-matrix least-squares methods based on F^2 using SHELXL-97, incorporated in the WINGX 1.64 crystallographic collective package.[24] For **1–3**, all non-hydrogen atoms were refined anisotropically. For **4**, except the chlorine and the four oxygens of a perchlorate ion, all the non-hydrogen atoms were refined anisotropically and those four oxygens were modeled satisfactorily with isotropic displacement parameters, displaced over two positions with a probability of 60 : 40. All the perchlorate Cl–O distances were restrained to obtain reasonable bond distances. Except for **1** (the hydrogen atoms are located from the difference Fourier map), the positions of the hydrogen atoms were calculated assuming ideal geometries. A summary of the data collection and structure refinement information is provided in Table 1.

CCDC reference numbers 253143 (**1**), 253144 (**2**), 253145 (**3**) and 253146 (**4**).

For crystallographic data in CIF or other electronic format see DOI: 10.1039/b512086a

Table 1 Data collection and structure refinement parameters for $[(\mathrm{L}^2)\mathrm{Cu}^{\mathrm{I}}(\mathrm{MeCN})_2][\mathrm{ClO}_4]$ (**1**), $[(\mu\text{-}\mathrm{L}^1)\mathrm{Cu}^{\mathrm{II}}(\mu\text{-}\mathrm{O_2CMe})]_n$ (**2**), $[\{(\mathrm{L}^2)\mathrm{Cu}(\mu\text{-}\mathrm{OH})(\mathrm{OClO_3})\}_2]$ (**3**) and $[\{(\mathrm{L}^2)\mathrm{Cu}(\mathrm{dmf})(\mu\text{-}\mathrm{O_2CMe})\}_2][\mathrm{ClO_4}]_2\cdot\mathrm{dmf}\cdot0.5\mathrm{MeCO_2H}$ (**4**)

	1	**2**	**3**	**4**
Chemical formula	$C_{19}H_{19}N_5ClO_4Cu$	$C_{20}H_{18}N_6O_4Cu_2$	$C_{30}H_{28}N_6Cl_2O_{10}Cu_2$	$C_{44}H_{52}N_9Cl_2O_{16}Cu_2$
M	480.38	533.48	832.58	1160.93
Crystal colour, habit	Yellow, block-like	Dark blue, block-like	Dark blue, block-like	Bluish green, block-like
T/K	100(2)	100(2)	100(2)	100(2)
λ/Å	0.71073	0.71073	0.71073	0.71073
Crystal System	Triclinic	Orthorhombic	Monoclinic	Monoclinic
Crystal size/mm × mm × mm	0.2 × 0.2 × 0.1	0.3 × 0.2 × 0.2	0.3 × 0.2 × 0.2	0.3 × 0.2 × 0.2
Space group	P-1 (no. 2)	$Pcab$ (no. 61)	Cc (no. 9)	$P2_1$ (no. 4)
a/Å	10.823(5)	17.217(5)	7.571(5)	11.234(5)
b/Å	10.882(5)	6.420(5)	18.245(5)	23.253(5)
c/Å	11.290(5)	17.644(5)	23.845(5)	19.581(5)
α/°	117.244(5)	90.0	90.0	90.0
β/°	90.425(5)	90.0	95.334(5)	98.723(5)
γ/°	115.172(5)	90.0	90.0	90.0
V/Å^3	1035.6(8)	1950.2(17)	3280(2)	5056(3)
Z	2	4	4	4
d_{calcd}/g cm^{-3}	1.541	1.817	1.686	1.508
μ/mm^{-1}	1.220	2.225	1.527	1.023
No. reflns. collected	6951	11553	10814	26671
No. indep. reflns.	4924 ($R_{\mathrm{int}} = 0.0168$)	2358 ($R_{\mathrm{int}} = 0.0316$)	5357 ($R_{\mathrm{int}} = 0.0328$)	12404 ($R_{\mathrm{int}} = 0.0852$)
No. reflns. used [$I > 2\sigma(I)$]	4474	2101	5026	7788
No. param.	347	145	451	1277
Final R indices [$I > 2\sigma(I)$] R_1, wR_2	0.0324 (0.0866)	0.0322 (0.0892)	0.0321 (0.0683)	0.0765 (0.1636)
R indices (all data)	0.0354 (0.0886)	0.0366 (0.0922)	0.0344 (0.0691)	0.1271 (0.1882)
GOF on F^2	1.007	1.074	0.971	1.003

Results and discussion

Synthesis and properties of $[(L^2)Cu^I(MeCN)_2][ClO_4]$ (1)

The bidentate ligand L^2 was synthesized from the reaction between benzyl chloride and 3-(2-pyridyl)pyrazole (HL^1)[18a] in the presence of NaOH in benzene. The reaction of $[Cu(MeCN)_4][ClO_4]$[18] with L^2 in MeCN, under anaerobic conditions, affords the yellow complex $[(L^2)Cu(MeCN)_2][ClO_4]$ (**1**) in ~78% yield (Scheme 1). The presence of coordinated MeCN molecules in **1** is observed by an IR absorption at 2250 cm^{-1}. The presence of ionic perchlorate is observed at 1089 and 627 cm^{-1}. The solution-state structure of **1** was judged by ^1H NMR spectroscopy (see ESI†). Microanalytical and solution electrical conductivity data (Experimental) conform to the above formulation.

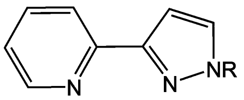
R = H (HL^1)
R = CH_2Ph (L^2)

$$L^2 + [Cu(MeCN)_4][ClO_4] \xrightarrow[25\ ^{\circ}C]{MeCN,\ -O_2} [(L^2)Cu^I(MeCN)_2][ClO_4]\ (\mathbf{1})$$

$$L^2 + [Cu(MeCN)_4][ClO_4] + O_2 + MeCO_2Et \xrightarrow[25\ ^{\circ}C]{MeCN\ /\ dmf,\ O_2} [(\mu\text{-}L^1)Cu^{II}(\mu\text{-}O_2CMe)]_n\ (\mathbf{2})$$

$$HL^1 + [Cu(H_2O)_6][ClO_4]_2 + Et_3N + MeCO_2Na \xrightarrow[25\ ^{\circ}C]{MeOH} (\mathbf{2})$$

$$L^2 + [Cu(MeCN)_4][ClO_4] \xrightarrow[25\ ^{\circ}C]{MeCN,\ O_2} [\{(L^2)Cu^{II}(\mu\text{-}OH)(OClO_3)\}_2]\ (\mathbf{3})$$

$$[\{(L^2)Cu^{II}(\mu\text{-}OH)(OClO_3)\}_2] + MeCO_2Et \xrightarrow[\sim 60\ ^{\circ}C]{dmf} [\{(L^2)Cu^{II}(dmf)(\mu\text{-}O_2CMe)\}_2][ClO_4]_2{\cdot}dmf{\cdot}0.5MeCO_2H\ (\mathbf{4})$$

Scheme 1

Crystal structure of $[(L^2)Cu^I(MeCN)_2][ClO_4]$ (1)

In order to confirm the identity of the copper(I) complex single crystal X-ray structure determination was carried out on **1**. A perspective view of the cationic part of the complex, with atom-labeling scheme is shown in Fig. 1. Selected metric parameters associated with the copper(I) center in **1** are given in Table 2. The structure of the ligand L^2 and its bidentate coordination mode are confirmed. The structure of **1** shows a distorted tetrahedral CuN_4 geometry around copper(I), provided by the coordination of the ligand and two MeCN molecules (Fig. 1). In fact, N–Cu–N angles span the range 79.60(6)–125.96(6)°, substantially deviating from the ideal tetrahedral angle. As expected, the dihedral angle between the N_1CuN_2 and N_4CuN_5 planes is 83.533(58)°, deviating from the ideal 90°. There are two types of heterocyclic nitrogen donor atoms in L^2: one pyrazole N(2) and one pyridine N(1). Interestingly, the Cu–N_{pz} (pz = pyrazole) bond length is shorter than that of Cu–N_{py} (py = pyridine). For both a triangular copper(I) complex of tris[3-(2-pyridyl)pyrazol-1-yl]hydroborate[25a] and a dimeric copper(I) complex with two bidentate pyrazolyl-pyridine arms attached to a thiophosphinate head-group,[25b] similar trends were observed. The average Cu–N_{MeCN} bond length of 1.9535(17) Å is comparable to that found for $[Cu(H_2CPZ_2)(MeCN)_2][ClO_4]$ [H_2CPZ_2 = bis(pyrazol-1-yl)methane].[13] The planar nature of pyridylpyrazole unit of L^2 is revealed by the angle between the two heterocyclic rings (~3°). To our knowledge, complex **1** is the first structurally characterized tetracoordinated bisacetonitrile copper(I) complex with a bidentate pyrazolyl-pyridine ligand.[13]

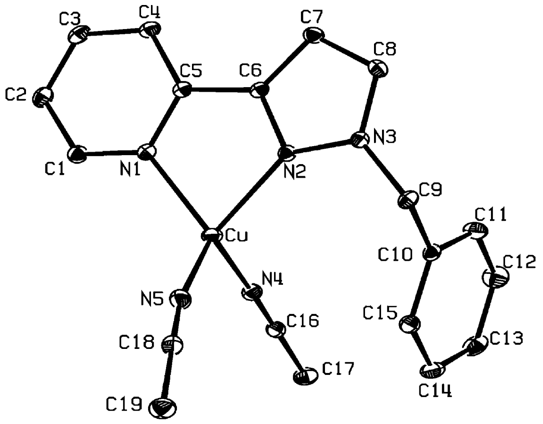

Fig. 1 View of $[(L^2)Cu(MeCN)_2]^+$ in the structure of (**1**). Hydrogen atoms are omitted for clarity.

Reactivity of 1 towards dioxygen and concomitant debenzylation of L^2 and hydrolysis of ethyl acetate: synthesis and properties of $[(\mu\text{-}L^1)Cu^{II}(\mu\text{-}O_2CMe)]_n$ (2)

The reaction between **1** and dioxygen was quite slow in MeCN. To enhance the rate of reaction, the solvent was removed from solution-generated **1**, and the residue was dissolved in dmf. Vapour diffusion of $MeCO_2Et$ into this solution afforded, after about a month, dark blue single crystals of polymeric (see below) $[(\mu\text{-}L^1)Cu(\mu\text{-}O_2CMe)]_n$ (**2**) in ~26% yield (Scheme 1). The designed synthesis of compound **2** was achieved in good yield (~74%) by direct reaction between $[Cu(H_2O)_6][ClO_4]_2$, HL^1, Et_3N and $MeCO_2Na$ in MeOH (Scheme 1). Notably, during the reaction conditions followed for the synthesis of **2** (*Method A*), debenzylation of L^2 (generating the deprotonated form of HL^1) and hydrolysis of $MeCO_2Et$ (generating the $MeCO_2^-$ ion) have occurred (see below). Microanalytical data (Experimental) conform to the above formulation. X-Ray structural analysis (see below) authenticated the structure and composition of **2**.

The IR bands at 1608 cm^{-1} and 1378 cm^{-1} are assigned to the stretching modes of the monoatomic acetate bridge in **2**.[26] Owing to the presence of the asymmetric bonding mode of the monoatomic acetate bridge, a large splitting ($\Delta = 230\ cm^{-1}$) of the –COO stretching frequencies is observed.[26] The electronic spectrum of polymeric copper(II) compound **2**, measured (190–1000 nm) in the solid state (dispersed in mineral oil mull), displays a broad absorption at 645 nm, justifying its dark blue colour.

In keeping with the EPR spectral behaviour of weakly exchange-coupled copper(II) dimers[27] solid samples of **2** display at 120 K a signal at $g = 4.23$ and a major absorption at $g = 2.16$, with minor absorptions on either side of this signal ($g = 2.90$, 1.86 and 1.76). The spectral feature is displayed in the ESI†. Minor absorptions are expected to be due to a lowering of copper(II) site symmetry. In fact, the EPR signal at $g = 4$ (due to $\Delta M_s = \pm 2$ transition) for copper(II) complexes is considered as a signature of the dimeric varieties.[27]

Table 2 Selected bond distances (Å) and angles (°) of $[(L^2)Cu^I(MeCN)_2][ClO_4]$ (**1**), $[(L^1)Cu^{II}(O_2CMe)]_n$ (**2**), $[\{(L^2)Cu(\mu\text{-}OH)(OClO_3)\}_2]$ (**3**) and $[\{(L^2)Cu^{II}(dmf)(\mu\text{-}O_2CMe)\}_2][ClO_4]_2\cdot dmf\cdot 0.5MeCO_2H$ (**4**)

1			
Cu–N(1)	2.0716(16)	N(1)–Cu–N(2)	79.60(6)
Cu–N(2)	2.0588(15)	N(1)–Cu–N(4)	111.74(6)
Cu–N(4)	1.9651(17)	N(1)–Cu–N(5)	125.96(6)
Cu–N(5)	1.9418(17)	N(2)–Cu–N(4)	115.54(7)
		N(2)–Cu–N(5)	113.55(6)
		N(4)–Cu–N(5)	108.23(7)
2			
Cu–N(1)	2.0332(19)	N(1)–Cu–N(2)	80.48(8)
Cu–N(2)	1.986(2)	N(1)–Cu–N(3)	169.98(8)
Cu–N(3)	1.9709(19)	N(1)–Cu–O(1)	92.04(8)
Cu–O(1)	1.9625(19)	N(1)–Cu–O(1′)	90.16(7)
Cu–O(1′)	2.3737(17)	N(2)–Cu–N(3)	97.85(9)
Cu–Cu′ (acetate-bridged)	3.3418(4)	N(2)–Cu–O(1)	171.95(7)
Cu–Cu′ (pyrazolate-bridged)	3.9232(4)	N(2)–Cu–O(1′)	97.32(8)
		N(3)–Cu–O(1)	90.03(8)
		N(3)–Cu–O(1′)	99.85(7)
		O(1)–Cu–O(1′)	79.60(7)
		Cu–O(1)–Cu′	100.40(7)
3			
Cu(1)–N(1)	1.999(3)	N(1)–Cu(1)–N(2)	80.75(12)
Cu(1)–N(2)	2.024(3)	N(1)–Cu(1)–O(1)	174.24(12)
Cu(1)–O(1)	1.915(2)	N(1)–Cu(1)–O(2)	95.58(11)
Cu(1)–O(2)	1.931(2)	N(2)–Cu(1)–O(1)	99.67(11)
Cu(2)–N(5)	2.018(3)	N(2)–Cu(1)–O(2)	171.77(11)
Cu(2)–N(6)	1.992(3)	N(5)–Cu(2)–N(6)	80.28(13)
Cu(2)–O(1)	1.923(2)	N(5)–Cu(2)–O(1)	100.60(10)
Cu(2)–O(2)	1.933(2)	N(5)–Cu(2)–O(2)	173.62(11)
Cu(1)–Cu(2)	2.8474(9)	N(6)–Cu(2)–O(1)	169.56(12)
		N(6)–Cu(2)–O(2)	95.44(11)
		O(1)–Cu(1)–O(2)	84.73(10)
		O(1)–Cu(2)–O(2)	84.47(10)
		Cu(1)–O(1)–Cu(2)	95.78(11)
		Cu(1)–O(2)–Cu(2)	94.95(10)
4			
Cu(1)–N(1)	2.037(8)	N(1)–Cu(1)–N(2)	80.1(4)
Cu(1)–N(2)	2.028(11)	N(1)–Cu(1)–O(1)	98.7(3)
Cu(1)–O(1)	2.183(7)	N(1)–Cu(1)–O(2)	170.8(3)
Cu(1)–O(2)	1.939(7)	N(1)–Cu(1)–O(6)	92.0(3)
Cu(1)–O(6)	1.946(8)	N(2)–Cu(1)–O(1)	96.9(4)
Cu(2)–N(4)	2.017(11)	N(2)–Cu(1)–O(2)	95.2(4)
Cu(2)–N(5)	2.010(8)	N(2)–Cu(1)–O(6)	169.7(3)
Cu(2)–O(3)	1.980(7)	O(1)–Cu(1)–O(2)	89.7(3)
Cu(2)–O(4)	2.135(8)	O(1)–Cu(1)–O(6)	90.7(3)
Cu(2)–O(5)	1.941(8)	O(2)–Cu(1)–O(6)	91.6(3)
Cu(1)–Cu(2)	3.0988(26)	N(4)–Cu(2)–N(5)	79.9(4)
Cu(1A)–N(1A)	2.001(19)	N(4)–Cu(2)–O(3)	92.6(3)
Cu(1A)–N(2A)	2.075(16)	N(4)–Cu(2)–O(4)	96.4(4)
Cu(1A)–O(1A)	2.34(3)	N(4)–Cu(2)–O(5)	168.7(4)
Cu(1A)–O(2A)	1.919(12)	N(5)–Cu(2)–O(3)	165.2(4)
Cu(1A)–O(6A)	1.960(8)	N(5)–Cu(2)–O(4)	100.9(3)
Cu(2A)–N(4A)	2.010(10)	N(5)–Cu(2)–O(5)	95.7(3)
Cu(2A)–N(5A)	2.018(11)	O(3)–Cu(2)–O(4)	92.5(3)
Cu(2A)–O(3A)	1.932(9)	O(3)–Cu(2)–O(5)	89.3(3)
Cu(2A)–O(4A)	2.176(8)	O(4)–Cu(2)–O(5)	94.6(3)
Cu(2A)–O(5A)	1.946(9)	N(1A)–Cu(1A)–N(2A)	77.8(8)
Cu(1A)–Cu(2A)	3.0792(29)	N(1A)–Cu(1A)–O(1A)	93.1(6)
		N(1A)–Cu(1A)–O(2A)	165.4(4)
		N(1A)–Cu(1A)–O(6A)	92.4(5)
		N(2A)–Cu(1A)–O(1A)	98.4(5)
		N(2A)–Cu(1A)–O(2A)	96.3(7)
		N(2A)–Cu(1A)–O(6A)	168.3(7)
		O(1A)–Cu(1A)–O(2A)	101.0(5)
		O(1A)–Cu(1A)–O(6A)	88.5(4)
		O(2A)–Cu(1A)–O(6A)	91.6(4)
		O(3A)–Cu(2A)–O(4A)	92.2(4)
		O(3A)–Cu(2A)–O(5A)	90.4(4)
		N(4A)–Cu(2A)–N(5A)	80.1(4)
		N(4A)–Cu(2A)–O(3A)	93.3(4)
		N(4A)–Cu(2A)–O(4A)	99.0(3)
		N(4A)–Cu(2A)–O(5A)	167.0(4)
		N(5A)–Cu(2A)–O(3A)	171.7(4)
		N(5A)–Cu(2A)–O(4A)	93.8(4)
		N(5A)–Cu(2A)–O(5A)	95.1(4)
		O(3A)–Cu(2A)–O(4A)	92.2(3)
		O(3A)–Cu(2A)–O(5A)	90.4(3)
		O(4A)–Cu(2A)–O(5A)	93.4(3)

Crystal structure of 2

A perspective view of the compound, with atom-labeling scheme is shown in Fig. 2. Table 2 contains the pertinent bond distances and bond angles. A part of the molecule is related to the other by a crystallographically imposed inversion centre. X-Ray analysis revealed three noteworthy features: (i) it is a polymeric copper(II) compound, (ii) debenzylation of the ligand L^2 has occurred, under our reaction conditions, and the 3-(2-pyridyl)pyrazolate ion (HL^1) thus formed acts as a bridging unit, in its deprotonated form, holding two metal centres[25b,28] and (iii) two kinds of bridge (acetate and pyrazolate) are present in the binuclear unit. Each Cu(II) ion is in a slightly distorted square pyramidal geometry ($\tau = 0.033$)[29] with coordination by two bridging pyrazolate nitrogen atoms N(2) and N(3), a pyridyl N(1) from a pyridylpyrazole unit, and an acetate coordination O(1) in the equatorial plane. An additional acetate, symmetry related to O(1), which is in a monodentate bridging mode,[30] provides axial coordination. It is a dinuclear copper(II) complex in which a near-planar $\{Cu_2(\mu\text{-}L^1)_2\}^{2+}$ core is present, as observed before.[25b,31] However, it has additional acetate bridging as well. Notably, the Cu–O–Cu′ bridges are dissimilar: Cu–O(1) 1.9625(19) and Cu–O(1)′ 2.3737(17) Å; the Cu–O(1)–Cu′ angle 100.40(7)° (Table 2). As in **1** the Cu–N$_{pz}$ bond distance is shorter than that of the Cu–N$_{py}$ distance. This must be due to the stereo-electronic requirement of the copper(II) ion. The Cu···Cu separations are 3.342 Å (acetate bridged)[30a,b] and 3.923 Å (pyrazolate bridged),[31] comparable to that reported in the literature. The observed Cu–O(bridging acetate)[30a,b] and Cu–N(bridging pyrazolate)[31] distances are comparable to that reported for complexes with similar structural motif. Although the acetato-bridged $\{Cu_2(\mu\text{-}O_2CMe)_2\}^{2+}$ and pyrazolato-bridged $\{Cu_2(\mu\text{-}C_3N_2)_2\}^{2+}$ dimeric units are each planar; they make an angle of 83.055(36)° with respect to each other. The Cu–N$_{py}$ and Cu–N$_{pz}$ bond lengths are normal.[1a,13,32]

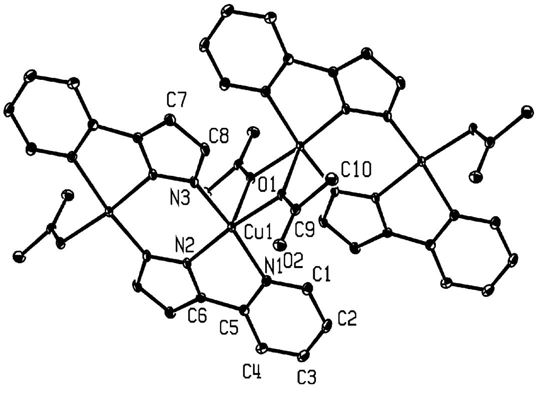

Fig. 2 View of the structure of $[(\mu\text{-}L^1)Cu(\mu\text{-}O_2CMe)]_n$ (**2**). Hydrogen atoms are omitted for clarity. Unlabeled atoms are related to labeled atoms by an inversion centre. Symmetry operations: (1) $-x, -y, -z + 1$; (2) $-x, -y + 1, -z + 1$.

Magnetism of 2

The magnetic behaviour of compound **2** is clearly of interest owing to the status of this complex as an example of the presence of both acetate- and pyrazolate-bridging between the copper(II) centers with distorted square pyramidal geometry. Such complexes are well known to exhibit antiferromagnetic/ferromagnetic exchange coupling between the metal centres[1a,30a,b,33] and accordingly the temperature-dependent (54–300 K) magnetic measurements on powdered samples of **2** were performed. The effective magnetic moment per copper (μ_{eff}/Cu) at 300 K was found to be 1.69 μ_B. A plot of $\chi_M T$ *versus* T for **2** (Fig. 3a) is typical of a moderate antiferromagnetically coupled dicopper(II) complex. The experimentally observed χ_M values (per dimer) were fitted to the Bleaney–Bowers equation,[34] suitably modified,[6c,d,g,12,35] based on the Heisenberg–Dirac–van Vleck, spin Hamiltonian ($\hat{H} = -2JS_1{\cdot}S_2$, in which the exchange parameter J is negative for antiferromagnetic and positive for ferromagnetic interaction), eqn (1), allowing for the presence of

$$\chi_M = 2Ng^2\beta^2/3k(T - \theta)[1 + 1/3\exp(-2J/kT)]^{-1}(1 - \rho) + (Ng^2\beta^2/2kT)\rho + 2N_\alpha \quad (1)$$

monomeric copper(II) impurity behaving as a Curie paramagnet, where ρ is the mole fraction of such an impurity, where N_α is the temperature-independent paramagnetism. A corrective term (θ) was incorporated for interdimer interactions.[35] The singlet–triplet energy gap is expressed in terms of $2J$ and other symbols have their usual meanings. Keeping N_α fixed at 60×10^{-6} cm^3 mol^{-1}, J, g, and θ parameters were determined by minimizing $R = \Sigma(\chi_m^{obs} - \chi_m^{calc})^2/\Sigma(\chi_m^{obs})^2$ using eqn (1), which gave good data fits. As shown by

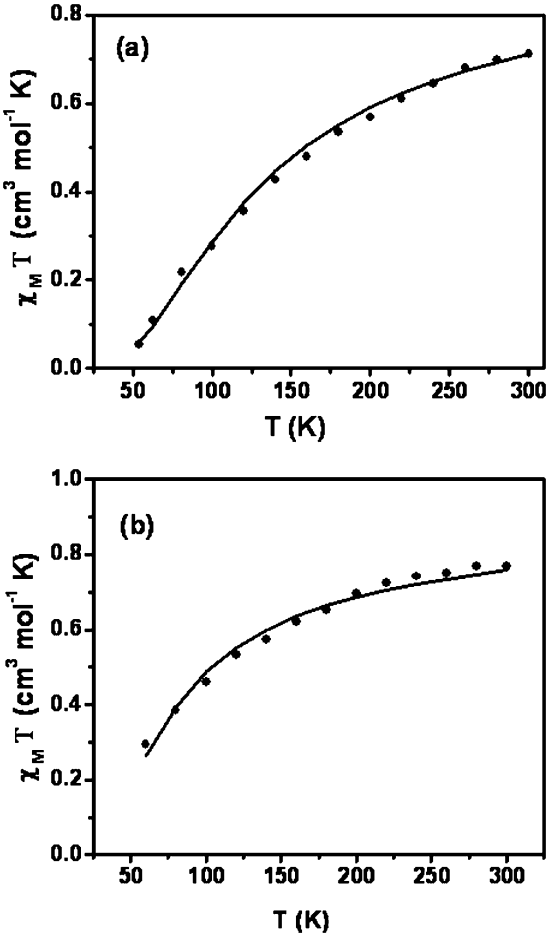

Fig. 3 Plot of $\chi_M T$ *vs.* T (●) for powdered samples of (a) $[\{(L^1)Cu(O_2CMe)\}_n]$ (**2**) and (b) $[\{(L^2)Cu(dmf)(\mu\text{-}O_2CMe)\}_2][ClO_4]_2{\cdot}dmf{\cdot}0.5MeCO_2H$ (**4**·dmf·0.5MeCO$_2$H). The solid lines represent the best simulated fit using the equation described in the text.

the trace in Fig. 3a, an excellent simulation (non-linear regression analyses)[6c,d,g] of the data could be attained with the following parameters: $J = -79$ cm^{-1}, $g = 2.15$, $\rho = 0.006$, $\theta = -0.18$ K and $R = 2.74 \times 10^{-7}$.

Given the reported results on the acetate-bridged (single-atom bridge through one of the oxygen atoms of an acetate)[1a,30a,b] and pyrazolate-bridged[1a,33] compounds the magnitude of the exchange interaction deserves a special attention. It has been well documented that in pyrazolate-bridged complexes (the primary pathway for the magnetic interaction must be through pyrazolate-bridges) the extent of antiferromagnetic coupling is larger when the coordination of the copper(II) ions is planar or square pyramidal. On the contrary, for the copper(II) compounds having acetate bridging mode as in **2** the magnetic exchange coupling is expected to be antiferromagnetic. In **2**, the Cu–O–Cu′ bridge angle of 100.40(7)° corresponds to an antiferromagnetic interaction (see below). The angle of 83.055(36)° between acetate-bridged $\{Cu_2(\mu\text{-}O_2CMe)_2\}^{2+}$ and pyrazolate-bridged $\{Cu_2(\mu\text{-}C_3N_2)_2\}^{2+}$ dimeric units is expected to reduce the extent of antiferromagnetism.[1a,33]

Reaction of 1 with dioxygen: synthesis and properties of $[\{(L^2)Cu(\mu\text{-}OH)(OClO_3)\}_2]$ (3)

To provide a rationale for the synthesis of **2** we set out for isolation of (i) a hydroxo-bound copper(II) compound from the reaction between **1** and dioxygen and (ii) a discrete diacetato-bridged copper(II) compound. Thus, exposure of a MeCN solution of **1** to dioxygen generated a green solution. Slow evaporation of this solution, after discarding an insoluble yellowish green polymeric material, in the presence of Et_2O led to the isolation of blue crystals of $[\{(L^2)Cu(\mu\text{-}OH)(OClO_3)\}_2]$ (**3**), within 2–3 days in ~43% yield (Scheme 1). Microanalytical data (Experimental) conform to the above formulation. X-ray structural analysis (see below) authenticated the structure and composition of **3**.

The IR spectra of **3** displays a sharp band at 3555 cm^{-1}, assignable to the stretching vibration of the hydroxo-bridge. For **3** the observed split absorption at 1106 cm^{-1} is suggestive of weakly coordinated ClO_4^- ions[36] (see below). The dark blue MeCN solution of **3** exhibits a band at 648 nm associated with a d–d transition of a square-based copper(II) centre.[37] A strong transition at 295 nm is also observed, which could be assigned to be due to $OH^- \rightarrow Cu(II)$ charge-transfer (ESI†).

The EPR spectrum for solid samples of **3** (Fig. 4) is of interest. This spectrum is typical of a triplet state with an axial zero-field splitting parameter D larger than the value of the incident quantum.[38,39] If the g and D tensors were coincident, their principal values could be deduced from the resonant fields by Wasserman's equations.[40] Notably, the EPR spectrum of **4** is very similar to that for $[\{(bpy)Cu^{II}(\mu\text{-}OH)\}_2][SO_4]\cdot 5H_2O$ (bpy = 2,2′-bipyridine).[39a] To interpret the EPR result we have made two assumptions: (i) the zero-field splitting parameter E is so small as to be considered equal to zero and (ii) the feature at about 3000 G resulted from the monomeric paramagnetic impurity. Although we used very pure samples but band-shape and temperature-dependent (300 K and 120 K) studies do not conflict with this assignment. Barnes *et al.*[39a] and Wasson *et al.*[39b] were able to support a similar assignment of a similar band on the basis of the temperature dependence of the peak intensities. With the aid of the copper(II) bipyridine[39a] and copper(II) cyanoacetate[39b] analysis and using the equations of Wasserman *et al.*[40] with the above approximations, our experimental spectra may be interpreted as follows. The major band at 7150 G is assigned to the high-field perpendicular transition. The band at 1600 G results from either the $\Delta M_s = \pm 2$ or the low-field parallel transition. In order to approximate the value of $|D|$, we have assumed, following Barnes *et al.*,[39a] $g_\perp$ to equal 2.05 and 2.10 (temperature-dependent magnetic data fitting analysis of **3** gave a $g = 2.12$, see below) and then have used these values of $g_\perp$ with the known value of $H_\perp$, to calculate $|D|$. We determine a relatively large zero-field splitting parameter of $D = 1.150$ ($g_\perp = 2.05$) or 1.222 ($g_\perp = 2.10$). The corresponding values for the bipyridine system were $D = 0.761$ ($g_\perp = 2.05$) or 0.813 ($g_\perp = 2.10$).[39a]

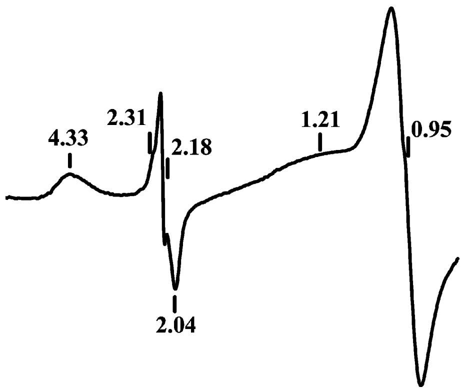

Fig. 4 EPR spectrum of $[\{(L^2)Cu(\mu\text{-}OH)(OClO_3)\}_2]$ (**3**) (solid) at 120 K.

Crystal structure of 3

A perspective view of **3**, with atom-labeling scheme is shown in Fig. 5. Table 2 contains the essential bond distances and bond angles. X-Ray crystallography established that it has the binuclear structure. The geometry at each copper(II) centre is best described as grossly square planar, with two oxygen atoms of the bridging hydroxo groups and two nitrogen atoms of the bidentate ligand L^2.

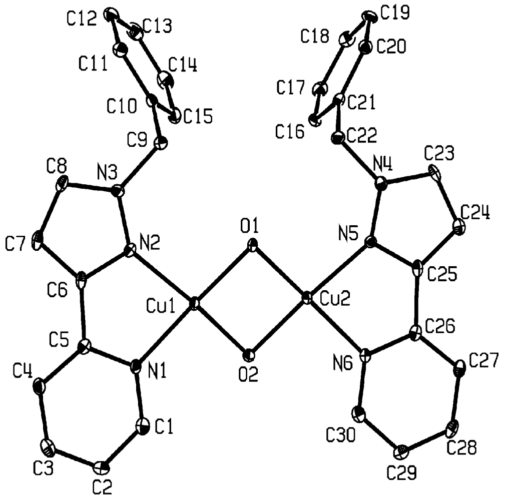

Fig. 5 View of $[\{(L^2)Cu(\mu\text{-}OH)\}_2]^{2+}$ in the structure of (**3**). Perchlorate coordinations are not shown for clarity. Hydrogen atoms are omitted for clarity.

In addition to the four strong equatorial ligands, each copper(II) ion is semi-coordinated[13,41a] to two oxygens of bridging perchlorate ions [Cu(1)–O(3) 2.7187(31), Cu(1)–O(7) 2.6988(28), Cu(2)–O(5) 2.5882(26), Cu(2)–O(9) 2.6175(27) Å]. The axial sites are at an average distance of 2.7088(30) Å at Cu(1) and 2.6029(27) Å at Cu(2), thereby completing a distorted octahedron around each copper(II) center. The pyridine and pyrazole rings of L^2 are almost planar, the angles being 2.46(0.12)° and 5.87(0.13)° for two ligands. Notably, the Cu–OH distances [Cu(1)–O(1) 1.915(2), Cu(1)–O(2) 1.931(2), Cu(2)–O(1) 1.923(2), Cu(2)–O(2) 1.933(2) Å] and Cu–O(H)–Cu angles [Cu(1)–O(1)–Cu(2) 95.78(11) and Cu(1)–O(2)–Cu(2) 94.95(10)°] are asymmetric. The distorted geometry at each copper(II) centre is revealed from the following considerations as well. The dihedral angles between the planes N(1)–Cu(1)–N(2) and O(1)–Cu(1)–O(2) and N(5)–Cu(2)–N(6) and O(1)–Cu(2)–O(2) are 9.83(10) and 11.92(11)°, respectively. However, the dihedral angle between the planes O(1)–Cu(1)–O(2) and O(1)–Cu(2)–O(2) is 2.41(10)°, implying more or less planar Cu_2O_2 core, presumably resulting mainly from the bridging perchlorate anions. The Cu···Cu separation is 2.8474(9) Å, comparable to that reported for a ferromagnetically coupled system.[41b] The Cu–N_{py} and Cu–N_{pz} distances are normal.[1a,13,32] In contrast to that observed in the structures of **1** and **2** in the present complex the average Cu–N_{py} distance is shorter than that of the Cu–N_{pz} distance. This is presumably as a consequence of the 'plasticity effect' due to the Jahn–Teller active copper(II) ion.[32b] The formation of di-μ-hydroxo-bridged dicopper(II) compounds due to the reaction between copper(I) compounds and dioxygen is a well known phenomenon.[1a,11–13,15] However, compound **3** joins a family of di-μ-hydroxo-bridged dicopper(II) compounds with terminal bidentate N-coordination,[5,15] synthesized following the reaction conditions used in this work. Compound **3** represents, to our knowledge, the first compound with such a core structure having terminal bidentate pyrazole/pyridine coordination.

Magnetism of 3

The molecular structure of **3** meets the requirements (average Cu–O(H)–Cu angle: 95.37°) of it to exhibit a ferromagnetic behaviour. According to Hodgson and Hatfield correlation[38a] for square-based di-μ-hydroxo-bridged dicopper(II) compounds[41] when the Cu–O–Cu angle is larger than 97.55°, the overall magnetic behavior is antiferromagnetic and for smaller values a ferromagnetic coupling is observed. At a Cu–O–Cu angle of 97.55° the singlet–triplet splitting energy ($2J$) would amount to zero. The magnetic susceptibility of the complex **3**, measured in the range $5 < T < 300$ K, is depicted in Fig. 6.

The magnetic behaviour of the complex is depicted in Fig. 6 in the form of $\chi_M T$ *versus* T, and shows a medium ferromagnetic interaction. At 300 K the $\chi_M T$ starts at a value of 0.95 cm^3 mol^{-1} ($\mu_{Cu} = 1.95\ \mu_B$) and increases to 0.97 cm^3 mol^{-1} ($\mu_{Cu} = 1.97\ \mu_B$) at about 200 K and to 100 K at 1.03 cm^3 mol^{-1} ($\mu_{Cu} = 2.03\ \mu_B$) and maximizes to 1.11 cm^3 mol^{-1} ($\mu_{Cu} = 2.11\ \mu_B$) at about 30 K. Below this temperature, the $\chi_M T$ values diminish to a value of 1.08 cm^3 mol^{-1} ($\mu_{Cu} = 2.08\ \mu_B$), which may originate from intermolecular antiferromagnetic interactions, or from zero-field splitting of the $S = 1$ state of the dinuclear species.[13,14b,35,38a] As shown by the trace in Fig. 6, an excellent simulation of the data could be attained with eqn (1) with the following parameters: $J = 41$ cm^{-1}, $g = 2.12$, $\rho = 0.009$, TIP ($2N_\alpha = 120 \times 10^{-6}$) (fixed), $\theta = -0.20$ K, and $R = 1.58 \times 10^{-7}$. The magnitude of the exchange interaction is similar to that observed before for similar compounds.[38a,41b,d,e]

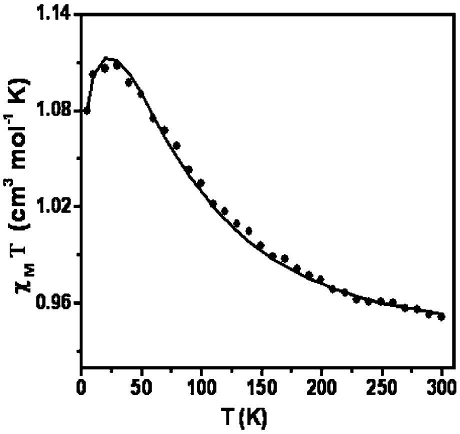

Fig. 6 Plot of $\chi_M T$ *vs.* T (●) for a powdered sample of $[\{(L^2)Cu(\mu\text{-}OH)(OClO_3)\}_2]$ (**3**). The solid line represents the best simulated fit using the equation described in the text.

Reaction of 3 with ethyl acetate: synthesis and properties of $[\{(L^2)Cu^{II}(dmf)(\mu\text{-}O_2CMe)\}_2][ClO_4]_2\cdot dmf\cdot 0.5MeCO_2H$ (4)

While an MeCN solution of **3** is blue, in dmf it generates a green solution. To such dmf solutions addition of $MeCO_2Et$ followed by warming (*ca.* 60 °C) for 4 h generated a bluish green solution. Cooling (*ca.* 24 h) of such solutions afforded light bluish green crystals of $[\{(L^2)Cu(dmf)(\mu\text{-}O_2CMe)\}_2][ClO_4]_2\cdot dmf\cdot 0.5MeCO_2H$ (**4**), in *ca.* 57% yield (Scheme 1). X-Ray structural analysis of **4** (see below) authenticated the structure and composition of this complex. Microanalytical and solution electrical conductivity data (Experimental) conform to the above formulation.

The ν_{as}(COO) and ν_s(COO) bands of **4** are at 1580 and 1439 cm^{-1}, respectively; the difference (140 cm^{-1}) is as expected for this chelated bridging mode of carboxylate coordination.[26] Light bluish green MeCN solutions of **4** displays a broad band at 718 nm due to a d–d transition with a shoulder at lower energy 964 nm (ESI†) indicating square-pyramidal geometry around copper(II).[37] The EPR spectrum of **4** is essentially unmodified between 120 K and 300 K. It is characteristic of a noncoupled copper(II) ion in a rhombic environment with three principal g values of 2.26, 2.13, and 2.03 (ESI†).[35,39]

Crystal structure of 4

In order to investigate whether or not Cu(II)-coordinated hydroxo groups in **3** are nucleophilic enough to bring about hydrolysis of $MeCO_2Et$ the X-ray structure determination of light bluish green solid **4** was undertaken. The elucidation of the crystal structure of **4** confirms that indeed hydrolysis of $MeCO_2Et$ has occurred. The structure of **4** reveals that it is a discrete molecule consisting of a dinuclear $[\{(L^2)Cu(dmf)(\mu\text{-}O_2CMe)\}_2]^{2+}$ cation (Fig. 7), two well-separated perchlorate anions, a dmf molecule, and half a molecule of $MeCO_2H$. The asymmetric unit contains two crystallographically independent molecules. Both dinuclear μ-1,3-acetato-bridged copper(II) complexes have essentially identical

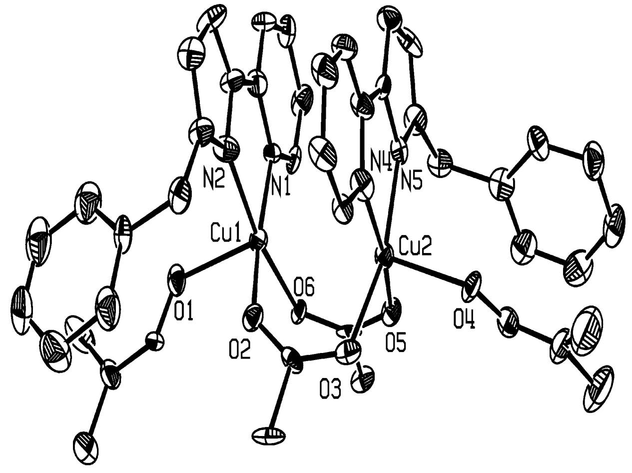

Fig. 7 View of $[\{(L^2)Cu(dmf)(\mu\text{-}O_2CMe)\}_2]^{2+}$ in the structure of (**4**). Hydrogen atoms are omitted for clarity.

coordination geometries, but the corresponding bond lengths and bond angles are different, to an appreciable extent (Table 2). Each copper(II) ion is coordinated by the ligand L^2 and a dmf molecule, and two copper(II) centers are bridged by two acetate groups. The cation represents the first example, to our knowledge, of a dinuclear copper(II) complex supported terminally by a bidentate N-donor ligand and bridged solely by two μ-1,3-acetate groups. It is to be noted that the acetate bridging mode present in **2** and **4** is different; **2** has comparatively rare monatomic bridging mode and **4** has the familiar bidentate $\eta^1{:}\eta^1{:}\mu_2$ bridging mode. Notably, out of two bridging acetate groups one is coordinated in a more asymmetric manner (Table 2). The coordination by dmf molecules is also asymmetric. As a consequence, the coordination geometries of the two copper(II) ions and the Cu · · · Cu distances in each dinuclear unit are different. Based on the structural index parameter τ, the geometry at Cu(1) ($\tau = 0.02$)/Cu(1A) ($\tau = 0.06$) and Cu(2) ($\tau = 0.05$)/Cu(2A) ($\tau = 0.08$) is best described as a slightly distorted square pyramidal,[29] with dmf oxygens O(1)/O(4) and O(1A)/O(4A) at the apex. In line with the structures of **1** and **2** in the present complex the average Cu–N_{pz} distance is shorter than that of the Cu–N_{py} distance.

In contrast to **3** having bis-hydroxo bridge between two copper(II) centres [Cu · · · Cu distance: 2.8474(9) Å], the bis-μ-1,3-acetato-bridged dicopper(II) complex induces much longer Cu · · · Cu distances of 3.0792(29) and 3.0988(26) Å in **4**. It is to be noted that during the synthesis of **2** (dmf/$MeCO_2Et$, 25 °C) decomposition of L^2 occurred but during the synthesis of **4** (dmf/$MeCO_2Et$, ~60 °C) the ligand L^2 remained intact. We are not in a position to provide an explanation for this behaviour.

Magnetism of 4

Variable-temperature magnetic susceptibility data were collected on powdered samples of complex **4** in the temperature range 60–300 K. The μ_{eff}/Cu decreases gradually from 1.82 μ_B at 300 K to a minimum of 1.08 μ_B at 60 K. A plot of $\chi_M T$ *versus* T for **4** (Fig. 3b) is typical of a moderate antiferromagnetically coupled dicopper(II) complex. Ignoring θ dependence and keeping g and $2N_\alpha$ fixed at 2.1 [typical value for a tetragonal Cu(II)] and 120×10^{-6} cm^3 mol^{-1}, the J and parameters were determined by minimizing $R = \Sigma(\chi_m^{obs} - \chi_m^{calc})^2/\Sigma(\chi_m^{obs})^2$ using eqn (1), which gave good data fits. An excellent simulation of the data could be attained with the following parameters: $J = -48$ cm^{-1} and $\rho = 0.016$, $R = 6.81 \times 10^{-7}$ (Fig. 3b).

The synthetic reactions, debenzylation of L^2 and ethyl acetate hydrolysis

Given the successful synthesis of compounds **2**, **3** and **4** (Scheme 1) an attempt has been made here (i) to clarify the synthetic reactions—mainly their stoichiometry, (ii) to provide a possible cause of debenzylation of L^2 and (iii) to provide a possible mechanism for the observed ethyl acetate hydrolysis.

It is believed that the dioxygen reaction with mononuclear Cu(I) complexes proceeds generally in steps leading to a 2e$^-$ reduced peroxo intermediate $\{Cu^{II}\text{–}(O_2)\text{–}Cu\}^{2+}$ [or its isomeric bis-oxo species $\{Cu^{III}\text{–}(O)_2\text{–}Cu^{III}\}^{2+}$].[4,5] The peroxide disproportionation, equivalent to the further reaction of $\{Cu^{II}\text{–}(O_2)\text{–}Cu^{II}\}^{2+}$ with Cu(I), leading to an overall reaction stoichiometry of Cu/O_2 = 4 : 1 is a possibility. Thus, the most common reaction of Cu(I) complexes with O_2 is this 4e$^-$ reduction and O–O cleavage reaction to give oxo "$Cu^{II}{}_2O$" species, which after reaction with H_2O eventually generates bis-hydroxy "$Cu^{II}{}_2(OH)_2$" products.[11] In the absence of definitive kinetic/mechanistic information it appears that the reaction stoichiometry for the formation of **3** follows a similar behaviour (Scheme 2). It should be noted, however, that the origin of the hydroxyl proton was not determined (residual water present in MeCN is a definite possibility).

The following reaction sequence for the synthesis of **4** from **3** firmly establishes that the degradation of ethyl acetate is due to Cu(II)-coordinated hydroxide ion and not by any reactive Cu(II)-coordinated peroxide species. The loosely bound ClO_4^- ions in **3** are replaced easily by coordinating solvent dmf, making the solvent exchangeable (with substrate) site(s) available. This condition allows $MeCO_2Et$ to bind to the copper(II) centre(s). Subsequent attack by the OH^- ion (nucleophile) bound to Cu(II) ion causes the hydrolysis of this unactivated ester. This justifies the reaction stoichiometry for the formation of **4** from **3** (Scheme 2). Although we do not have any proof for the formation of EtOH

$$4[(L^2)Cu^{I}(MeCN)_2][ClO_4]\ (\mathbf{1}) + O_2 + H_2O\ (\text{in MeCN / dmf}) + MeCO_2Et \longrightarrow [\{(\mu\text{–}L^1)Cu^{II}(\mu\text{–}O_2CMe)\}_n]\ (\mathbf{2})$$

$$4[(L^2)Cu^{I}(MeCN)_2][ClO_4]\ (\mathbf{1}) + O_2 + 2H_2O\ (\text{in MeCN}) \longrightarrow 2[\{(L^2)Cu^{II}(\mu\text{–}OH)(OClO_3)\}_2]\ (\mathbf{3})$$

$$[\{(L^2)Cu^{II}(\mu\text{–}OH)(OClO_3)\}_2]\ (\mathbf{3}) + 2MeCO_2Et\ (\text{in dmf}) \longrightarrow [\{(L^2)Cu^{II}(dmf)(\mu\text{–}O_2CMe)\}_2][ClO_4]_2{\cdot}dmf{\cdot}0.5MeCO_2H\ (\mathbf{4}) + 2EtOH$$

Scheme 2

(Scheme 2), it is reasonable to assume its formation given literature reports (see below).[17b]

The synthesis of **2** (*Method A*, Experimental; Scheme 1) with concomitant debenzylation of L^2 and hydrolysis of ethyl acetate deserves special attention. Due to the complexity of the reactions involved and the results available to hand we are not in a position to provide a stoichiometric reaction for the synthesis of **2** (Scheme 2). However, the following reaction sequence provides a rationale for the observed hydrolysis of ethyl acetate. Reaction of complex **1** with O_2, the formation/decomposition of copper–dioxygen intermediate, subsequent formation of bis-hydroxy species and nucleophilic attack of Cu(II)-coordinated hydroxide ion to ethyl acetate, generating acetate ion as in the formation of **4** from **3** (*vide supra*, Scheme 2) is a reasonable hypothesis.

A commonly observed result of decomposition of Cu/O_2 complexes of tridentate N-donor ligands (2-pyridylalkylamine[11b] or triazacyclononane[4h]) bearing a benzyl pendant arm is oxidative N-debenzylation (intramolecular oxidation of C–H bonds that are "activated" due to their position α to an amine donor and/or a phenyl ring) to yield a secondary amine and an aldehyde or ketone. Given the reaction conditions (oxygenation at 25 °C, sluggish nature, low yield of **2**; Experimental, *Method A*) adopted in the synthesis of **2** we rule out the possibility that a thermally unstable copper-bound peroxide intermediate, formed due to the reaction of compound **1** and O_2 in air, might have attacked the benzylic position of L^2 effecting debenzylation of L^2.[4h,11b] The debenzylation of L^2 results in liberation of one equivalent of HL^1 into the medium per molecule of L^2 and deprotonated HL^1 acts as a bridging ligand, as observed in the polymeric compound **2**. Solvolysis/hydrolysis reactions of 3-(2-pyridyl)pyrazole-based polydentate ligands, including reactions of Cu(I) complexes and O_2, have literature precedence.[25b,28b,42]

It is worth noting the findings of two reports pertinent to this work. (i) Using solution-generated OH^- bound mononuclear copper(II) compounds Chin and co-workers reported efficient hydrolysis of methyl acetate (pH 7.0; 25 °C), following kinetic experiments.[16] (ii) Karlin and co-workers reported[17b] hydrolysis of $MeCO_2Et$ forming acetate ion, which ended up bridging two copper(II) centres, by an alkoxo-bridged dicopper(II) compound with a terminally coordinated hydroxide ion, suggested (mass spectral proof) to be present in solution when structurally characterized tetranuclear singly hydroxo-bridged copper(II) complex (dimer-of-dimer type) was dissolved in MeCN. During $MeCO_2Et$ hydrolysis the formation of acetic acid[16b] and other byproduct alcohol[17b] were previously observed. Therefore, it is interesting to note the presence of half a molecule of $MeCO_2H$ in the asymmetric unit of **4** (see above). The reactivity of a dihydroxo-bridged dicopper(II) compound towards hydrolysis of $MeCO_2Et$, to our knowledge, is unprecedented. Although numerous structurally characterized bis(μ-hydroxo)dicopper(II) complexes terminally coordinated by bidentate N-donor ligands are known,[1a,11–13,15,38a,41] compound **3** is unique in its reactivity behaviour. The results presented here show that it is the subtle combination of the ligand electronic/steric effect and the presence of suitable bridging ligands to hold two metal ions in correct distance for substrate to get bound and metal-bound hydroxide ion to act as the nucleophile to bring about hydrolysis of the unactivated ester $MeCO_2Et$. The intramolecular attack by a hydroxide ion, coordinated to one copper(II) centre and serving as the nucleophile, on the carbon atom of the $MeCO_2Et$ is expected to have occurred, as is known from elegant metalloenzyme hydrolytic model studies,[9,10] including copper(II) complexes.[16,17]

Concluding remarks

In conclusion, we have succeeded in preparing a mononuclear copper(I), a polymeric acetato-/pyrazolato-bridged copper(II) and two discrete dihydroxo-/diacetatato-bridged copper(II) complexes, of a new bidentate pyrazolyl-pyridine ligand L^2, with a range of structural varieties at our disposal. Under mild conditions hydrolysis of the unactivated ester $MeCO_2Et$ has been achieved. During the synthesis of polymeric Cu(II) compound, debenzylation of L^2 has also been observed. Complex **3** serves as the key compound to bring about this unusual reaction and is proposed to occur by an intramolecular hydrolysis mechanism. Thus **3** can be regarded as a functional model for the hydrolytic enzymes, pertinent to the assignment of possible mechanisms for ester hydrolysis catalyzed by enzymes.[8–10] We plan to probe further the reactivity of **3** toward other substrates (however, it does not react with phosphate esters) and mechanistic aspects of the chemistry reported here. The three copper(II) complexes provide a variable bridge which in turn led to a range of $Cu\cdots Cu$ distances. Temperature-dependent magnetic studies have revealed the existence of both ferromagnetic and antiferromagnetic exchange coupling in this family of dicopper(II) compounds. We plan to carry out detailed temperature-dependent EPR studies on the ferromagnetically coupled compound **2**.

Acknowledgements

We thank the Council of Scientific & Industrial Research and the Department of Science and Technology, New Delhi for financial support. We sincerely thank Dr V. Balamurugan and Mr Akhilesh K. Singh for their help in the preparation of this manuscript. Comments of the reviewers were very helpful at the revision stage.

References

1 (*a*) R. Mukherjee, in *Comprehensive Coordination Chemistry-II: From Biology to Nanotechnology*, chapter on copper, ed. J. A. McCleverty and T. J. Meyer, vol. ed. D. E. Fenton, Elsevier/Pergamon, Amsterdam, 2004, vol. 6, pp. 747–910; (*b*) R. Mukherjee, *Indian J. Chem.*, 2003, **42A**, 2175.
2 (*a*) R. H. Holm, P. Kennepohl and E. I. Solomon, *Chem. Rev.*, 1996, **96**, 2239; (*b*) E. I. Solomon, U. M. Sundaram and T. E. Machonkin, *Chem. Rev.*, 1996, **96**, 2563.
3 E. I. Solomon, P. Chen, M. Metz, S.-K. Lee and A. E. Palmer, *Angew. Chem., Int. Ed.*, 2001, **40**, 4570.
4 (*a*) K. D. Karlin and Z. Tyeklár, *Adv. Inorg. Biochem.*, 1994, **9**, 123; (*b*) K. D. Karlin and A. D. Zuberbühler, in *Bioinorganic Catalysis*, ed.J. Reedijk and E. Bouwman, Marcel Dekker, Inc., New York, 1999, 469; (*c*) H.-C. Liang, M. Dahan and K. D. Karlin, *Curr. Opin. Chem. Biol.*, 1999, **3**, 168 and references therein; (*d*) N. Kitajima and Y. Moro-oka, *Chem. Rev.*, 1994, **94**, 737; (*e*) A. G. Blackman and W. B. Tolman, *Struct. Bonding (Berlin)*, 2000, **97**, 179; (*f*) S. Schindler, *Eur. J. Inorg. Chem.*, 2000, 2311; (*g*) S. Itoh and S. Fukuzumi, *Bull. Chem. Soc. Jpn.*, 2002, **75**, 2081; (*h*) E. A. Lewis and W. B. Tolman, *Chem. Rev.*, 2004, **104**, 1047.
5 (*a*) V. Mahadevan, R. J. M. Klein Gebbink and T. D. P. Stack, *Curr. Opin. Chem. Biol.*, 2000, **4**, 228; (*b*) T. D. P. Stack, *Dalton Trans.*, 2003, 1881; (*c*) L. M. Mirica, X. Ottenwaelder and T. D. P. Stack, *Chem. Rev.*, 2004, **104**, 1013.

6 (*a*) D. Ghosh, T. K. Lal, S. Ghosh and R. Mukherjee, *Chem. Commun.*, 1996, 13; (*b*) D. Ghosh, T. K. Lal and R. Mukherjee, *Proc. Indian Acad. Sci. (Chem. Sci.)*, 1996, **108**, 251; (*c*) R. Gupta and R. Mukherjee, *Inorg. Chim. Acta*, 1997, **261**, 233; (*d*) D. Ghosh and R. Mukherjee, *Inorg. Chem.*, 1998, **37**, 6597; (*e*) R. Gupta, D. Ghosh and R. Mukherjee, *Proc. Indian Acad. Sci. (Chem. Sci.)*, 2000, **112**, 179; (*f*) R. Gupta and R. Mukherjee, *Tetrahedron Lett.*, 2000, **41**, 7763; (*g*) S. P. Foxon, D. Utz, J. Astner, S. Schindler, F. Thaler, F. W. Heinemann, G. Liehr, J. Mukherjee, V. Balamurugan, D. Ghosh and R. Mukherjee, *Dalton Trans.*, 2004, 2321.

7 J. Mukherjee and R. Mukherjee, *Inorg. Chim. Acta*, 2002, **337**, 429.

8 (*a*) W. N. Lipscomb and N. Sträter, *Chem. Rev.*, 1996, **96**, 2375; (*b*) N. Sträter, W. N. Lipscomb, T. Klabunde and B. Krebs, *Angew. Chem., Int. Ed.*, 1996, **35**, 2024.

9 (*a*) M. A. Halcrow and G. Christou, *Chem. Rev.*, 1994, **94**, 2421; (*b*) D. E. Wilcox, *Chem. Rev.*, 1996, **96**, 2435; (*c*) G. C. Dismukes, *Chem. Rev.*, 1996, **96**, 2909.

10 (*a*) J. Chin, *Acc. Chem. Res.*, 1991, **24**, 145; (*b*) N. H. Williams, B. Takasaki, M. Wall and J. Chin, *Acc. Chem. Res.*, 1999, **32**, 485.

11 (*a*) K. D. Karlin and Y. Gultneh, *Prog. Inorg. Chem.*, 1987, **35**, 219; (*b*) I. Sanyal, M. Mahroof-Tahir, M. S. Nasir, P. Ghosh, B. I. Cohen, Y. Gultneh, R. W. Cruse, A. Farooq, K. D. Karlin, S. Liu and J. Zubieta, *Inorg. Chem.*, 1992, **31**, 4322.

12 D. Rojas, A. M. García, A. Vega, Y. Moreno, D. Venegas-Yazigi, M. T. Garland and J. Manzur, *Inorg. Chem.*, 2004, **43**, 6324.

13 C.-C. Chou, C.-C. Su, H.-L. Tsai and K.-H. Lii, *Inorg. Chem.*, 2005, **44**, 628.

14 (*a*) J. Mukherjee, V. Balamurugan, M. S. Hundal and R. Mukherjee, *J. Chem. Sci.*, 2005, **117**, 111; (*b*) J. Mukherjee, R. Gupta, T. Mallah and R. Mukherjee, *Inorg. Chim. Acta*, 2005, **358**, 2711.

15 (*a*) S. Itoh, M. Taki, H. Nakao, P. L. Holland, W. B. Tolman, L. Que, Jr. and S. Fukuzumi, *Angew. Chem., Int. Ed.*, 2000, **39**, 398; (*b*) Y. Shimazaki, T. Nogami, F. Tani, A. Odani and O. Yamauchi, *Angew. Chem., Int. Ed.*, 2001, **40**, 3859; (*c*) D. J. E. Spencer, N. W. Aboelella, A. M. Reynolds, P. L. Holland and W. B. Tolman, *J. Am. Chem. Soc.*, 2002, **124**, 2108; (*d*) D. J. E. Spencer, A. M. Reynolds, P. L. Holland, B. A. Jazdzewski, C. Duboc-Toia, L. Le Pape, S. Yokota, Y. Tachi, S. Itoh and W. B. Tolman, *Inorg. Chem.*, 2002, **41**, 6307; (*e*) M. Taki, S. Teramae, S. Nagatomo, Y. Tachi, T. Kitagawa, S. Itoh and S. Fukuzumi, *J. Am. Chem. Soc.*, 2002, **124**, 6367; (*f*) L. M. Mirica, M. Vance, D. J. Rudd, B. Hedman, K. O. Hodgson, E. I. Solomon and T. D. P. Stack, *J. Am. Chem. Soc.*, 2002, **124**, 9332; (*g*) C. Shimokawa, S. Yokota, Y. Tachi, N. Nishiwaki, M. Ariga and S. Itoh, *Inorg. Chem.*, 2003, **42**, 8395; (*h*) A. P. Cole, V. Mahadevan, L. M. Mirica, X. Ottenwaelder and T. D. P. Stack, *Inorg. Chem.*, 2005, **44**, 7345.

16 (*a*) J. Chin and V. Jubian, *J. Chem. Soc., Chem. Commun.*, 1989, 839; (*b*) J. Chin and M. Banaszczyk, *J. Am. Chem. Soc.*, 1989, **111**, 2724.

17 (*a*) N. N. Murthy, M. Mahroof-Tahir and K. D. Karlin, *J. Am. Chem. Soc.*, 1993, **115**, 10404; (*b*) S. T. Frey, N. N. Murthy, S. T. Weinstraub, L. K. Thompson and K. D. Karlin, *Inorg. Chem.*, 1997, **36**, 956.

18 (*a*) A. J. Amoroso, A. M. C. Thompson, J. C. Jeffery, P. L. Jones, J. A. McCleverty and M. D. Ward, *J. Chem. Soc., Chem. Commun.*, 1994, 2751; (*b*) M. D. Ward, J. A. McCleverty and J. C. Jeffery, *Coord. Chem. Rev.*, 2001, **222**, 251.

19 H.-C. Liang, K. D. Karlin, R. Dyson, S. Kaderli, B. Jung and A. D. Zuberbühler, *Inorg. Chem.*, 2000, **39**, 5884.

20 W. J. Geary, *Coord. Chem. Rev.*, 1971, **7**, 81.

21 M. Ray, D. Ghosh, Z. Shirin and R. Mukherjee, *Inorg. Chem.*, 1997, **36**, 3568.

22 D. F. Evans, *J. Chem. Soc.*, 1959, 2003.

23 C. J. O'Connor, *Prog. Inorg. Chem.*, 1982, **29**, 203.

24 L. J. Farrugia, *WINGX version 1.64, An Integrated System of Windows Programs for the Solution, Refinement and Analysis of Single-Crystal X-ray Diffraction Data*, Department of Chemistry, University of Glasgow, 2003.

25 (*a*) P. L. Jones, J. C. Jefferey, J. P. Maher, J. A. McCleverty, P. H. Rieger and M. D. Ward, *Inorg. Chem.*, 1997, **36**, 3088; (*b*) J. S. Fleming, E. Psillakis, J. C. Jeffery, K. L. V. Mann, J. A. McCleverty and M. D. Ward, *Polyhedron*, 1998, **17**, 1705.

26 G. B. Deacon and R. J. Phillips, *Coord. Chem. Rev.*, 1980, **33**, 227.

27 T. D. Smith and J. R. Pilbrow, *Coord. Chem. Rev.*, 1974, **13**, 173.

28 (*a*) P. L. Jones, J. C. Jeffery, J. A. McCleverty and M. D. Ward, *Polyhedron*, 1997, **16**, 1567; (*b*) R. L. Paul, S. M. Couchman, J. C. Jeffery, J. A. McCleverty, Z. R. Reeves and M. D. Ward, *J. Chem. Soc., Dalton Trans.*, 2000, 845.

29 A. W. Addison, T. N. Rao, J. Reedijk, J. van Rijn and G. C. Verschoor, *J. Chem. Soc., Dalton Trans.*, 1984, 1349 (square pyramidal geometry $\tau = 0$; trigonal bipyramidal geometry $\tau = 1$).

30 (*a*) A. M. Greenaway, C. J. O'Connor, J. W. Overman and E. Sinn, *Inorg. Chem.*, 1981, **20**, 1508; (*b*) J.-P. Costes, F. Dahan and J.-P. Laurent, *Inorg. Chem.*, 1985, **24**, 1018; (*c*) G. K. Patra, G. Mostafa, D. A. Tocher and D. Datta, *Inorg. Chem. Commun.*, 2000, **3**, 56.

31 (*a*) J. Pons, A. Chadghan, A. Alvarez-Larena, J. F. Piniella and J. Ros, *Inorg. Chem. Commun.*, 2001, **4**, 610; (*b*) M. J. Hallam, C. A. Kilner and M. A. Halcrow, *Acta Crystallogr., Sect. C*, 2002, **C58**, m445.

32 (*a*) R. Mukherjee, *Coord. Chem. Rev.*, 2000, **203**, 151; (*b*) R. Gupta, T. K. Lal and R. Mukherjee, *Polyhedron*, 2002, **21**, 1245.

33 (*a*) H. Matsushima, H. Hamada, K. Watanabe, M. Koikawa and T. Tokii, *J. Chem. Soc., Dalton Trans.*, 1999, 971; (*b*) E. Spodine, A. M. Atria, J. Valenzuela, J. Jalocha, J. Manzur, A. M. García, M. T. Garland, O. Peña and J.-Y. Saillard, *J. Chem. Soc., Dalton Trans.*, 1999, 3029.

34 Bleaney and K. D. Bowers, *Proc. R. Soc. London, A*, 1952, **214**, 451.

35 J. Comarmond, P. Plumeré, J.-M. Lehn, Y. Agnus, R. Louis, R. Weiss, O. Kahn and I. Morgenstern-Badarau, *J. Am. Chem. Soc.*, 1982, **104**, 6330.

36 (*a*) S. F. Pavkovic and D. W. Meek, *Inorg. Chem.*, 1965, **4**, 1091; (*b*) M. R. Rosenthal, *J. Chem. Educ.*, 1973, **50**, 331.

37 B. J. Hathaway, in *Comprehensive Coordination Chemistry*, ed. G. Wilkinson, R. D. Gillard and J. A. McCleverty, vol. 5, pp. 533–594, Pergamon Press, Oxford, 1987 and references therein.

38 (*a*) V. H. Crawford, H. W. Richardson, J. R. Wasson, D. J. Hodgson and W. E. Hatfield, *Inorg. Chem.*, 1976, **15**, 2107; (*b*) H. P. Berends and D. W. Stephan, *Inorg. Chem.*, 1987, **26**, 749.

39 (*a*) J. A. Barnes, D. J. Hodgson and W. E. Hatfield, *Inorg. Chem.*, 1972, **11**, 144; (*b*) J. R. Wasson, C.-I. Shyr and C. Trapp, *Inorg. Chem.*, 1968, **7**, 469.

40 E. Wasserman, L. C. Snyder and W. A. Yager, *J. Chem. Phys.*, 1964, **41**, 1763.

41 (*a*) S. A. Komaei, G. A. van Albada, J. G. Haasnoot, H. Kooijman, A. L. Spek and J. Reedijk, *Inorg. Chim. Acta*, 1999, **286**, 24; (*b*) G. A. van Albada, I. Mutikainen, U. Turpeinen and J. Reedijk, *Inorg. Chim. Acta*, 2001, **324**, 273; (*c*) G. A. van Albada, I. Mutikainen, W. J. J. Smeets, A. L. Spek, U. Turpeinen and J. Reedijk, *Inorg. Chim. Acta*, 2002, **327**, 134; (*d*) S. Youngme, G. A. van Albada, O. Roubeau, C. Pakawatchai, N. Chaichit and J. Reedijk, *Inorg. Chim. Acta*, 2003, **342**, 48; (*e*) S. Youngme, C. Chailuecha, G. A. van Albada, C. Pakawatchai, N. Chaichit and J. Reedijk, *Inorg. Chim. Acta*, 2004, **357**, 2532.

42 K. Locher, W. L. Driessen and J. Reedijk, *Inorg. Chim. Acta*, 1987, **127**, 135.